

## Article

# Isolation and Characterization of Compounds from *Ochreinauclea maingayi* (Hook. f.) Ridsd. (Rubiaceae) with the Aid of LCMS/MS Molecular Networking

Norfaizah Osman<sup>1</sup>, Azeana Zahari<sup>1,2,\*</sup> , Hazrina Hazni<sup>2</sup> , Wan Nurul Nazneem Wan Othman<sup>3</sup>, Nurulfazlina Edayah Rasol<sup>3</sup>, Nor Hadiani Ismail<sup>3</sup>, Pierre Champy<sup>4</sup>, Mehdi A. Beniddir<sup>4</sup> , Marc Litaudon<sup>5</sup> , and Khalijah Awang<sup>1,2,\*</sup>

<sup>1</sup> Department of Chemistry, Faculty of Science, Universiti Malaya, Kuala Lumpur 50603, Malaysia

<sup>2</sup> Centre for Natural Products Research and Drug Discovery (CENAR), Level 3, Research Management & Innovation Complex, Universiti Malaya, Kuala Lumpur 50603, Malaysia

<sup>3</sup> Atta-ur-Rahman Institute for Natural Product Discovery, Level 9 FF3, Universiti Teknologi MARA Puncak Alam Campus, Bandar Puncak Alam 42300, Malaysia

<sup>4</sup> Équipe "Chimie des Substances Naturelles" BioCIS, CNRS, Université Paris-Saclay, 17 Avenue des Sciences, 91400 Orsay, France

<sup>5</sup> Institut de Chimie des Substances Naturelles, CNRS, UPR 2301, Université Paris-Saclay, 91198 Gif-sur-Yvette, France

\* Correspondence: azeanazahari@um.edu.my (A.Z.); khalijah@um.edu.my (K.A.); Tel.: +60-3-79674064 (A.Z.)

**Abstract:** Phytochemical investigation of the dichloromethane crude extract from the bark of *Ochreinauclea maingayi* with the aid of LCMS/MS-based molecular networking guided the isolation and accelerated the elucidation of known and new indole alkaloids. The molecular networking analysis produces two main clusters, along with 41 non-prioritized clusters and self-loop nodes. Each cluster has several nodes which depict the fractions contained within those nodes. An implementation of a fraction mapping for each node represents the molecular weight and key fragment data of each compound. From the analysis of each cluster and node, we can deduce the indole alkaloids are the scaffold of interest. Indole scaffold can be found between F5 and F10 that contain several types of indole alkaloids. In total, we have successfully purified nine indole alkaloids, including 9H- $\beta$ -carboline-4-carboxylate **2**, norharmane **3**, harmane **4**, naucleidine **10**, neonaucleine **15**, 1,2,3,4-tetranorharmane-1-one **16**, naulafine **19**, cadambine **9**, and a new monoterpene indole alkaloid dihydrodeglycocadambine **7** from F5 to F10 using a chromatographic technique. Their structures were confirmed by 1D-NMR, 2D-NMR, UV, IR, LCMS, and MS2LDA. Several clusters and nodes contain ions that could not be annotated, suggesting that they may possess novel compounds that are yet to be discovered.

**Keywords:** indole alkaloid; molecular networking; dereplication; Rubiaceae; *Ochreinauclea maingayi*



**Citation:** Osman, N.; Zahari, A.; Hazni, H.; Wan Othman, W.N.N.; Rasol, N.E.; Ismail, N.H.; Champy, P.; Beniddir, M.A.; Litaudon, M.; Awang, K. Isolation and Characterization of Compounds from *Ochreinauclea maingayi* (Hook. f.) Ridsd. (Rubiaceae) with the Aid of LCMS/MS Molecular Networking. *Separations* **2023**, *10*, 74. <https://doi.org/10.3390/separations10020074>

Academic Editor: Marcello Locatelli

Received: 24 December 2022

Revised: 9 January 2023

Accepted: 12 January 2023

Published: 21 January 2023



**Copyright:** © 2023 by the authors. Licensee MDPI, Basel, Switzerland. This article is an open access article distributed under the terms and conditions of the Creative Commons Attribution (CC BY) license (<https://creativecommons.org/licenses/by/4.0/>).

## 1. Introduction

Natural product studies usually deal with samples of complex chemical mixtures. Isolation and structural elucidation of the metabolites within these mixtures remain tedious and time-consuming despite the advanced performance of modern chromatographic and analytical technologies. Dereplication is one of the strategies to prioritize metabolites by having efficient isolation and elucidation using LC-MS/MS-based molecular networking (MN). Using the literature and an annotated molecular network as a guide, it significantly reduces the cost of drug discovery pipeline by increasing the speed of isolation of new and known compounds. Hence, in this study, we describe the use of a targeted substructure-informed molecular networking screening approach to detect indole alkaloid (IA) scaffold and predict the molecular structure of possible compounds that are present. IA are biosynthesized from tryptophan which undergo decarboxylation to form tryptamine. This is

followed by the Mannich reaction of the latter and secologanin to produce strictosidine, which serves as the precursor in the production of indole alkaloids [1,2]. IA can be found in Apocynaceae, Icacinaceae, Nyssaceae, Gelsemiaceae, Loganiceae, and Rubiaceae which have been known to exhibit various bioactivities [3–5]. In the framework of the scientific collaboration between the ICSN and the Universiti Malaya, our laboratories have embarked on a project to find IA scaffold using MN from *Ochreinauclea maingayi*, which belongs to the genus of *Ochreinauclea* (Rubiaceae). Throughout the world, there are only two species, *O. maingayi* and *O. missionis*, which are understudied in phytochemical analysis [6,7]. *O. maingayi* is a commercial timber that is mostly distributed in Peninsular Malaysia, Borneo, Sumatra, and Thailand [8,9]. The bark root of *O. missionis*, which is typically discovered in India, has been used to treat ulcers, fever, rheumatism, jaundice, edema, hepatitis, and haemophilia [6,7]. Prior phytochemical studies of the leaves of *O. maingayi* [10] revealed that indole alkaloids are the predominant compounds and are active towards vasorelaxant activities. In this study, we report the chemical constituents, particularly indole alkaloids, in the bark from this plant.

First, the LC-MS/MS data of crude and fractions were acquired, then the .RAW data from LC-MS/MS were converted to .mzXML format using MSConvert (<http://proteowizard.sourceforge.net>, accessed on 4 March 2021). Every .mzXML file was processed using MZmine 2 v53 to produce the .mgf data [11]. The .mgf preclustered spectral data file and its corresponding.csv metadata file (for RT and integration) were exported and submitted to GNPS (Global Natural Product Social Molecular Networking). Next, a molecular network was constructed using a minimum cosine score value of 0.6 and a network topK of 10 with six match fragment ions, which indicated similarity in the MS/MS spectra. The generated molecular network can be viewed and analyzed using Cytoscape (ver 3.8.2). To further prove this analysis, MS2LDA decomposes the fragmentation spectra into blocks of co-occurring fragments and losses, referred to as “Mass2Motifs” [12].

## 2. Materials and Methods

### 2.1. General Experimental Procedures

The analytical and preparative TLC was carried out on Merck 60 F254 silica gel plates (absorbent thickness of 0.25 and 0.50 mm, respectively). Column chromatography (CC) was performed using silica gel (Merck 230–400 mesh, ASTM). The IR spectra were recorded using a Perkin-Elmer Spectrum 400 FT-IR Spectrometer. The NMR spectra were acquired in CDCl<sub>3</sub>, C<sub>5</sub>D<sub>5</sub>N, and CD<sub>3</sub>OD (Merck, Germany) with tetramethyl silane as the internal standard (Merck, Germany) using the BRUKER Avance III 400 and BRUKER Avance III 600 spectrometers. The LC/MS profiling was identified using an UHPLC-Orbitrap MS. Nitrogen was used as the sheath and an auxiliary gas at a flow rate of 0.25 mL/min. The optimum source (ESI) condition was a spray voltage of 3500 V (4.5) and 2500V (3.7) kV under the positive mode, respectively; a S-Lens RF Level at 55.00; an ESI capillary temperature 325 °C; and a probe heater temperature at 40 °C. The UV spectra were recorded using a Shimadzu 1650 PC UV-Vis Spectrophotometer. An AP-300 Automatic Polarimeter was used to measure optical rotations. All solvents were of analytical grade and were distilled prior to use.

### 2.2. Plant Material

The stem bark of *O. maingayi* was collected from the Ulu Sat Reserve Forest, Machang, Kelantan, Malaysia. The plant was identified by Prof. Colin E. Ridsdale (Leiden University, Leiden, The Netherland), and a voucher specimen (KL 5595) is deposited with the Universiti Malaya herbarium.

### 2.3. Extraction

The dried and powdered stem barks of *O. maingayi* (2.0 kg) were extracted by cold extraction procedure using three different solvents, including hexane, dichloromethane (CH<sub>2</sub>Cl<sub>2</sub>), and methanol (CH<sub>3</sub>OH), to give three different crude extracts depending on

the polarity of the compounds. The dried grounded stem bark of *O. maingayi* was first treated with hexane (10 L) for three days at room temperature. The resulting slurry was filtered, and the residual plant material was moistened with 25% ammonia solution (1 L) and left for 2 h to aggregate the nitrogen-containing compounds in the plant. The basified residual plant material was then successively re-extracted with dichloromethane  $\text{CH}_2\text{Cl}_2$  (15 L, 3 $\times$ ). The  $\text{CH}_2\text{Cl}_2$  extract was repeatedly extracted with a solution of 5% hydrochloric acid (0.5 L, 1 $\times$ ) until it gave a negative result for the Mayer's test. It was next basified with 25% ammonia solution to about a pH of 11 and re-extracted with  $\text{CH}_2\text{Cl}_2$  (3 L, 1 $\times$ ) to yield 10 g of dark brown gummy  $\text{CH}_2\text{Cl}_2$  crude. The  $\text{CH}_2\text{Cl}_2$  extract (10 g) was subjected to silica gel column chromatography (CC) and eluted with  $\text{CH}_2\text{Cl}_2/\text{CH}_3\text{OH}$  (100:1 to 1:100, *v/v*) to yield 10 fractions.

#### 2.4. Purification of Compounds

Compounds **15** (3.2 mg,  $\text{CH}_2\text{Cl}_2$ :  $\text{CH}_3\text{OH}$ ; 99:1) and **16** (2.2 mg,  $\text{CH}_2\text{Cl}_2$ :  $\text{CH}_3\text{OH}$ ; 99:1) were obtained from F5 after purification using PTLC. Meanwhile, F6 yielded **19** (2.8 mg,  $\text{CH}_2\text{Cl}_2$ :  $\text{CH}_3\text{OH}$ ; 99:1) using PTLC. F7 was subjected to microcolumn eluted with  $\text{CH}_2\text{Cl}_2/\text{CH}_3\text{OH}$  (100:1 to 1:100, *v/v*) to give 5 fractions, and then fraction 5(1) was purified with PTLC to obtain **3** (1.6 mg,  $\text{CH}_2\text{Cl}_2$ :  $\text{CH}_3\text{OH}$ ; 99:1) and **4** (3.5 mg,  $\text{CH}_2\text{Cl}_2$ :  $\text{CH}_3\text{OH}$ ; 99:1). F8 was purified to afford compound **2** (2.3 mg,  $\text{CH}_2\text{Cl}_2$ :  $\text{CH}_3\text{OH}$ ; 98:2) using PTLC. Compound **10** (3.6 mg,  $\text{CH}_2\text{Cl}_2$ :  $\text{CH}_3\text{OH}$ ; 95:5) was obtained after the purification of F9 using PTLC. The purification of F10 by PTLC yielded **7** (6.0 mg,  $\text{CH}_2\text{Cl}_2$ :  $\text{CH}_3\text{OH}$ ; 94:6) and **9** (110.0 mg,  $\text{CH}_2\text{Cl}_2$ :  $\text{CH}_3\text{OH}$ ; 94:6), respectively.

#### 2.5. Data-Dependent LCMS Analysis, FBMN, and MS2LDA Parameters

##### 2.5.1. Data-Dependent LCMS Orbitrap MS/MS Analysis

For LC-MS analysis, the crude extracts were dissolved in LC-MS grade MeOH at a concentration of 0.1 mg/mL. The analyses were performed on a Thermo Scientific Orbitrap Fusion Tribrid. The samples were injected and chromatographically separated on an Accucore TM Vanquish  $\text{C}_{18+}$  Dim. (2.1  $\times$  100 mm) at a temperature of 40 °C with an injection volume of 1.0  $\mu\text{L}$ . The separation was achieved with a binary LC solvent system controlled by Mobile phase A consisting of 99.9% water/0.1% formic acid (LC/MS grade) and mobile phase B containing 100% MeOH (LC/MS grade), which were pumped at a rate 0.250 mL/min. According to the following gradient sequence of percentage Solvent B increment: maintained at 5% from 0 to 2 min, increased from 5 to 100% from 2 to 30 min, maintained at 100% until 40 min. MS/MS analysis was performed in positive mode, with the following optimized operating conditions: spray voltage, 3.5 (+) and 2.5 (-) kV; column temperature 40 °C; capillary temperature 325 °C; sheath gas flow rate (Arb): 50, auxiliary gas flow rate (Arb): 10; Sweep gas (Arb): 1; RF lens (%): 60; Scan range (*m/z*): 100–1000; Collision-induced dissociation (CID) energy was adjusted to 30%. All data were recorded and processed using Thermo Xcalibur software version 4.3.

##### 2.5.2. Feature-Based Molecular Networking

The MS2 data files were converted from the raw (Orbitrap) standard data format to .mzXML format using MSConvert Software, which is part of the ProteoWizard package [13]. All .mzXML files were then processed using MZmine 2 v53 [11]. The mass detection was realized by keeping the noise level at 5.0E5 at MS1 and at 5.0E4 at MS2. The ADAP chromatogram builder was used with a minimum group size of scan of 5, a group intensity threshold of 3.0E5, a minimum highest intensity of 3.0E5, and *m/z* tolerance of 0.001 Da (or 5 ppm). The ADAP wavelet deconvolution algorithm was used with the following standard setting: a chromatographic threshold = 1%, a search minimum in RT range min = 0.30, a minimum relative height = 1%, a minimum absolute height = 5.0E5, a minimum ratio peak top/edge = 2, and a peak duration range (min) = 0 to 2 min. The isotopologues were grouped using the isotopic peak grouper algorithm with a *m/z* tolerance of 0.006 Da (20 ppm) and a RT tolerance of 0.5 min. Peak alignment was performed using the join

aligner module ( $m/z$  tolerance of 0.001 Da (or 5 ppm), weight for RT = 2.0, and absolute RT tolerance 0.3 min). The feature list row filler peak  $m/z$  was 100 to 1000, which kept the MS2 scan and reset the ID. The peak list was gap filled with the same RT and  $m/z$  range gap filler module ( $m/z$  tolerance 0.001 or 5ppm). Eventually, the.mgf preclustered spectral data file and its corresponding.csv metadata file (for RT and integration) were exported using the dedicated “Export/Submit for GNPS/FBMN” option.

### 2.5.3. Molecular Networking Parameters

A molecular network was created using the online workflow (<https://ccms-ucsd.github.io/GNPSDocumentation/>, accessed on 16 August 2021) on the GNPS [14] website (<http://gnps.ucsd.edu>, accessed on 16 August 2021). The data were filtered by removing all MS/MS fragment ions within  $\pm 17$  Da of the precursor  $m/z$ . The MS/MS spectra were window filtered by choosing only the top 6 fragment ions in the  $\pm 50$ Da window throughout the spectrum. The precursor ion mass tolerance was set to 0.02 Da with a MS/MS fragment ion tolerance of 0.03 Da. A network was then created where the edges were filtered to have a cosine score above 0.6 and more than 6 matched peaks. Furthermore, the edges between two nodes were kept in the network if and only if each of the nodes appeared in the other's respective top 10 most similar nodes. Finally, the maximum size of a molecular family was set to 100, and the lowest scoring edges were removed from the molecular families until the molecular family size was below this threshold. All matches kept between the network spectra and the library spectra were required to have a score above 0.7 and at least 6 matched peaks. The spectra in the network were then searched against the GNPS spectral libraries. The molecular networking data were analysed and visualized using Cytoscape (ver 3.8.2) [15].

### 2.5.4. MS2LDA Unsupervised Substructure Annotation

The fragmentation spectra were mined for co-occurring fragments and neutral losses using the latent Diriclet allocation algorithm on the MS2LDA web app [16]. The following parameters were used for this task: isolation\_window (0.5), min\_ms2\_int (500), n\_its (1000), K (60), ms2\_bin (0.005 Da), and Zero MotifDB. The result of the MS2LDA annotation is publicly available at the following link: [https://ms2lda.org/basicviz/toggle\\_public/2353/](https://ms2lda.org/basicviz/toggle_public/2353/), accessed on 5 July 2022. The inspection and the annotation of the Mass2Motifs were realized using the MS2LDA.org Web app.

## 3. Results and Discussions

The present work aims to explore and highlight the existing link between the spectral molecular networks, the predicted fractions, and experimental fractions, and how we deduce isolation and elucidation of known and unknown compounds.

By using this molecular networking (MN), we could discover the presence of indole alkaloids in F5-F10. By exploiting the beneficial functions of MN, the conventional natural product isolation and identification workflow could be simplified via early dereplication, which saves time, effort, and cost. MN could provide an easy approach to identify each metabolite, including minor and major compounds, by evaluating their chromatographic retention times, chromatographic peak abundance, molecular formulas, and MS/MS spectral properties. Additionally, MS2LDA facilitates the validation of both known and new alkaloids by analyzing their fragmentation patterns.

Our strategy begins with analyzing the LC-MS<sup>2</sup> profile (Figure 1) of the dichloromethane CH<sub>2</sub>Cl<sub>2</sub> extract from the bark of *O.maingayi* under the positive ion mode. More than 1000 MS/MS spectra over the range  $m/z$  of 70 to 1000 were generated. The raw data of LCMS for the extract and ten fractions (fractionation of crude using column chromatography) were converted to .mgf, then mapping was performed using GNPS (<https://gnps.ucsd.edu/ProteoSAFe/status.jsp?task=54bf2f40092c41e28f69b60e845f056d> accessed on 16 August 2021)) to generate massive molecular networking (MN) (Figure 2). The MN contains two main clusters (A and B), along with 41 non-prioritized clusters and self-loop nodes.

Each cluster has several nodes which depict the fractions contained within those nodes. These nodes represent the molecular weight and key fragment data of each compound. From the analysis of each cluster and node, we can deduce the cluster that is of interest, which is indole alkaloids (IA) in this case. After analyzing the massive MN data (Table 1), we deduce five fractions (F5–F10) of interest containing several types of indole alkaloids. In total, we have successfully purified nine indole alkaloids (Figure 3) from F5 (neonaucline 15, 1,2,3,4-tetranorharmane-1-one 16 [10]), F6 (naulafine 19 [17]), F7 (norharmane 3 [18], harmane 4 [19]), F8 (methyl 9H- $\beta$ -carboline-4-carboxylate 2 [20]), F9 (naucleidine 10 [10]), and F10 (dihydrodeglycocadambine 7, cadambine 9 [21]). Compounds 2, 3, 4, 10, 15, 16, and 19 are non-isoprenoid tryptophan indole alkaloids, which are from the simple  $\beta$ -carboline (2, 3, 4, and 16), indolopyridine (10), nauclefine (15), and naulafine (19) types, while 7 and 9 are IA belonging to the cadambine type. Compound 7 is a new monoterpene indole alkaloid that has been successfully elucidated with the MS-guided purification.

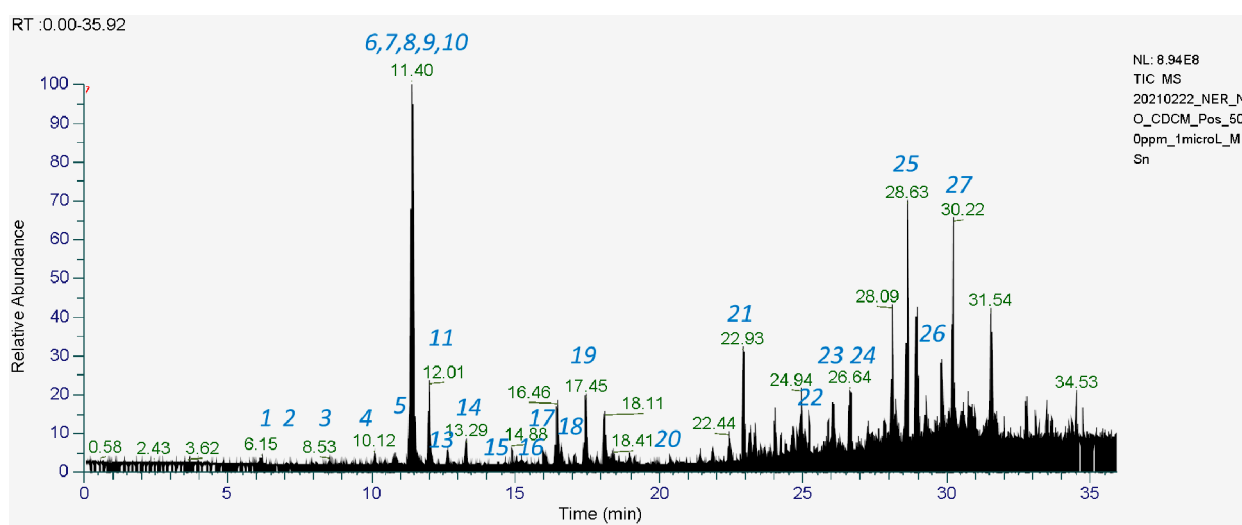


**Figure 1.** Dichloromethane crude extract of *Ochreinauclea maingayi* showing the LCMS profile under positive mode  $[M + H]^+$ .

Next, to further prove our elucidation on 7, we utilized the web-based MS2LDA [12,16] to process our MS/MS data and explore the results through interactive visualizations. This process indicated that Cluster A exhibits a Mass2motif (motif\_370) shared by 16 parent masses that possess IA scaffold. Out of these, two parent masses, Parent: 492 and Parent: 803, show characteristic fragmentation patterns belonging to IA scaffold [23]. The details of Parent: 492 and Parent: 803 MS/MS spectra, the protonated molecular ions, and the fragmentation pathway are shown in Figures 4 and 5, respectively. The analysis of Parent: 492 fragmentation pattern led to the identification of cadambine 9, while the analysis of Parent: 830 led to the discovery of the new compound dihydrodeglycocadambine 7.

Cadambine 9 (545.2153 Da) loses hexose sugar (162.075 Da) to give deglycocadambine 6 (383.1750 Da) [22]. With respect from this parent mass fragmentation that gives 6, we can deduce that the new IA compound isolated is dihydrodeglycocadambine 7 (385.177 Da) from the loss of hexose sugar at C-21 and a double bond at C16–C17, which has a similar pattern of fragmentation pathway as seen in cadambine 9 (Figure 4).

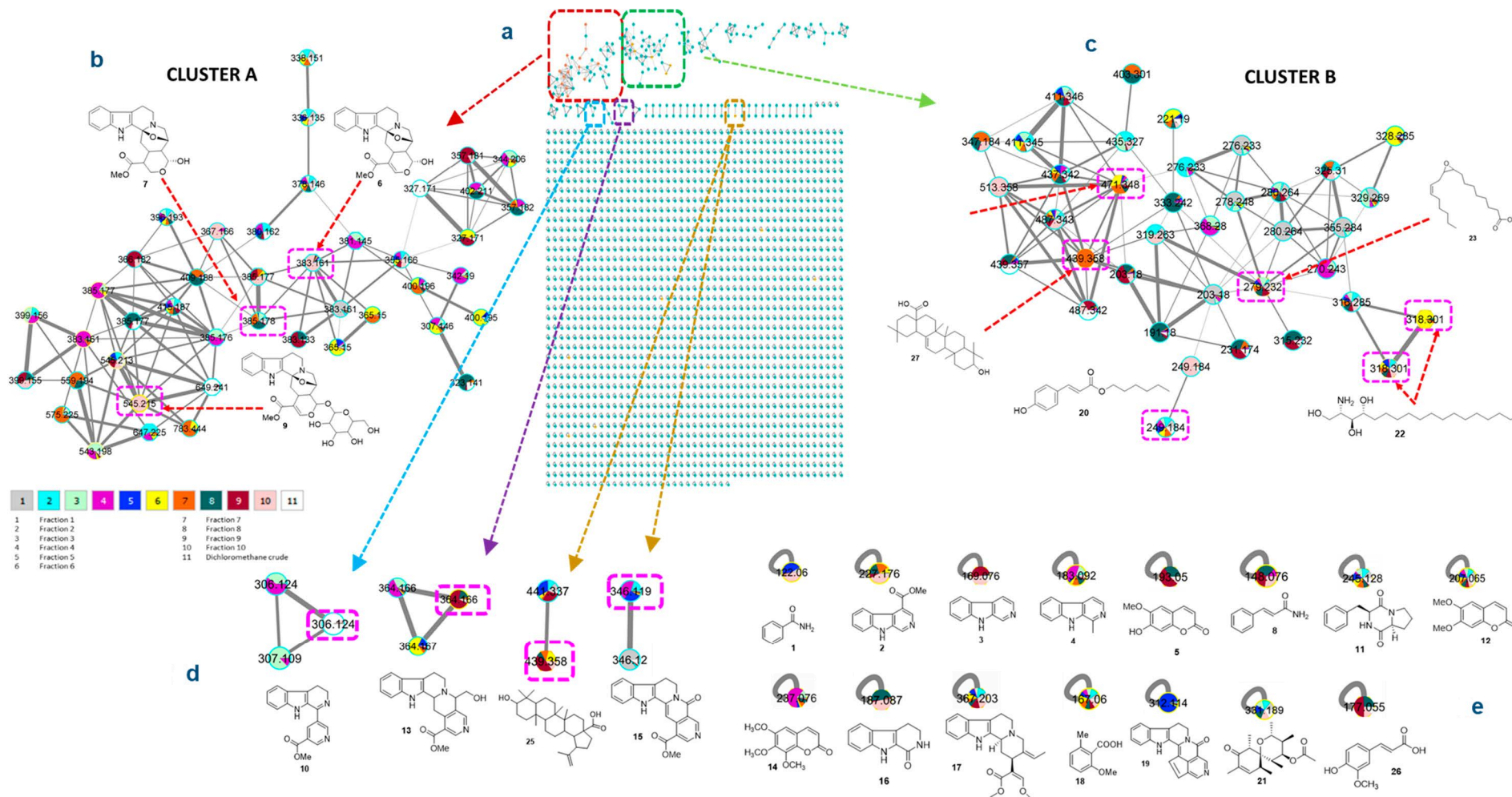


**Figure 2.** (a) Massive molecular networking of dichloromethane crude extract of the bark of *O. mainiyi* (b) Implementation of a fraction mapping for molecular networking-guided purification for cluster A. (c) Implementation of a fraction mapping for molecular networking-guided purification for cluster B. (d) Implementation of a fraction mapping for molecular networking-guided purification for non-prioritized clusters. (e) Implementation of a fraction mapping for molecular networking-guided purification for self-loop nodes.

**Table 1.** Chemical constituents identified in the dichloromethane crude extract of the bark of *O. maingayi*.

Peak No	Compound Identifications	Precursor Ion Mass (m/z)	Molecular Formula	RT Means (min)	Ion Type	Predicted Fractions (Figure 2)	Experimental Fraction	Key Fragment (m/z)
<b>IA (Cluster A, non-prioritized cluster and self-loops)</b>								
2	Methyl 9H- $\beta$ -carboline-4-carboxylate <sup>b</sup>	227.176	C <sub>13</sub> H <sub>11</sub> N <sub>2</sub> O <sub>2</sub>	7.03	[M + H] <sup>+</sup>	F10,F8,F9,F7,F5,F6	<b>F8</b>	209,100
3	Norharmane <sup>ab</sup>	169.076	C <sub>11</sub> H <sub>9</sub> N <sub>2</sub>	8.88	[M + H] <sup>+</sup>	F10,F9,F8,F5	F7	142,115
4	Harmane <sup>bc</sup>	183.091	C <sub>12</sub> H <sub>11</sub> N <sub>2</sub>	10.41	[M + H] <sup>+</sup>	F6,F7,F8,F9,F10,F1,F2,F3,F4	<b>F7</b>	142,115
6	Deglycocadambine <sup>d</sup>	383.161	C <sub>21</sub> H <sub>23</sub> N <sub>2</sub> O <sub>5</sub>	11.15	[M + H] <sup>+</sup>	F8,F9,F10,F7,F6,F4		365,337,305,183
7	Dehydrodeglycocadambine <sup>b</sup>	385.177	C <sub>21</sub> H <sub>25</sub> N <sub>2</sub> O <sub>5</sub>	11.23	[M + H] <sup>+</sup>	F8,F9, <b>F10</b>	<b>F10</b>	367,227,183,170,144
9	Cadambine <sup>b</sup>	545.215	C <sub>27</sub> H <sub>23</sub> N <sub>2</sub> O <sub>10</sub>	11.43	[M + H] <sup>+</sup>	F9, <b>F10</b>	<b>F10</b>	383,365,227,170,139
10	Naucedine <sup>bc</sup>	306.124	C <sub>18</sub> H <sub>16</sub> N <sub>3</sub> O <sub>2</sub>	11.75	[M + H] <sup>+</sup>	F10, <b>F9</b> ,F8,F6	<b>F9</b>	189,163,144
13	Cadamine <sup>c</sup>	364.167	C <sub>21</sub> H <sub>22</sub> N <sub>3</sub> O	13.2	[M + H] <sup>+</sup>	F6,F7,F5		346,317,285,233,144
15	Neonaucaline <sup>bc</sup>	346.119	C <sub>20</sub> H <sub>16</sub> N <sub>3</sub> O <sub>2</sub>	14.39	[M + H] <sup>+</sup>	F4, <b>F5</b> ,F2,F7,F6	<b>F5</b>	314,286,271,231
16	1,2,3,4-tetranorharmane-1-one <sup>ab</sup>	187.087	C <sub>11</sub> H <sub>11</sub> N <sub>2</sub> O	15.21	[M + H] <sup>+</sup>	F2,F8,F9,F10,F6,F4,F3	F5	158,142,130,115
17	Geissoschizine methyl ether <sup>a</sup>	367.203	C <sub>22</sub> H <sub>26</sub> N <sub>2</sub> O <sub>3</sub>	15.62	[M + H] <sup>+</sup>	F8,F9,F10		170,144,130,108,75
19	Naulafine <sup>b</sup>	312.114	C <sub>20</sub> H <sub>14</sub> N <sub>3</sub> O	17.15	[M + H] <sup>+</sup>	F5, <b>F6</b> ,F4,F8,F9,F10,F2,F4	<b>F6</b>	269,242,187,170,159,141, 116
<b>Triterpene (Cluster B and Self-loops)</b>								
23	Glycyrrhetic acid <sup>a</sup>	471.348	C <sub>30</sub> H <sub>47</sub> O <sub>4</sub>	26.57	[M + H] <sup>+</sup>	F6,F7,F5,F4,F1		189,175,133,119,107,95
25	Betulinic acid <sup>a</sup>	439.358	C <sub>30</sub> H <sub>46</sub> O <sub>2</sub>	28.72	[M + H] <sup>+</sup> -H <sub>2</sub> O	F9,F10, F7,F8,F6		393,259,243,213,179,137,95
27	Oleanolic acid <sup>a</sup>	439.358	C <sub>30</sub> H <sub>46</sub> O <sub>2</sub>	30.47	[M + H] <sup>+</sup> -H <sub>2</sub> O	F7,F8,F9,F10		215,203,189,147,133,119,107,95,81,69
<b>Coumarine (Self-loops)</b>								
5	Scopoletine <sup>ab</sup>	193.050	C <sub>10</sub> H <sub>9</sub> O <sub>4</sub>	10.75	[M + H] <sup>+</sup>	F4, <b>F3</b>	<b>F3</b>	150,133,122,94,77,66
12	Scoparone <sup>b</sup>	207.065	C <sub>11</sub> H <sub>11</sub> O <sub>4</sub>	12.73	[M + H] <sup>+</sup>	F1, <b>F2</b> ,F3,F4,F5,F6,F7,F8,F9	<b>F2</b>	163,151,146,135,118,107,91
14	Di-O-methylfraxetin <sup>a</sup>	237.076	C <sub>10</sub> H <sub>9</sub> O <sub>5</sub>	13.98	[M + H] <sup>+</sup>	F4,F3,F5,F7,F8		207,179,147,133,123,91

Table 1. Cont.

Peak No	Compound Identifications	Precursor Ion Mass (m/z)	Molecular Formula	RT Means (min)	Ion Type	Predicted Fractions (Figure 2)	Experimental Fraction	Key Fragment (m/z)
<b>Phenolic (Cluster B)</b>								
20	Hexyl- <i>p</i> coumarate <sup>b</sup>	249.184	C <sub>15</sub> H <sub>20</sub> O <sub>3</sub>	20.58	[M + H] <sup>+</sup>	F1,F2,F3,F4,F5,F6,F7,F10	F1	175,163,153,147,125,109,95,69
26	Trans ferulic acid <sup>a</sup>	177.055	C <sub>10</sub> H <sub>11</sub> O <sub>4</sub>	29.60	[M + H] <sup>+</sup>	F8,F9,F10		117,89,78
<b>Fatty acid (Cluster B)</b>								
24	9(10)-EpOME <sup>a</sup>	279.232	C <sub>18</sub> H <sub>33</sub> O <sub>3</sub>	26.59	[M + H] <sup>+</sup> -H <sub>2</sub> O	F8,F9,F10,F7,F1,F4,F5,F6		135,123,109,95,81,67
<b>Lipid (Cluster B)</b>								
22	Phytosphingosine <sup>a</sup>	318.301	C <sub>18</sub> H <sub>40</sub> NO <sub>3</sub>	25.11	[M + H] <sup>+</sup>	F6,F7,F2,F4,F5		300,282,270,252,95,83
<b>Organic acid (Self-loops)</b>								
11	cyclo(L-Phe-D-Pro) <sup>a</sup>	245.128	C <sub>14</sub> H <sub>17</sub> N <sub>2</sub> O <sub>2</sub>	11.90	[M + H] <sup>+</sup>	F3, F2,F1,F6,F5,F7,F8,F9,F4		154,120,98,70
18	2-Methoxy-6-methyl benzoic acid <sup>b</sup>	167.060	C <sub>9</sub> H <sub>11</sub> O <sub>3</sub>	17.11	[M + H] <sup>+</sup>	F1,F2,F3,F4,F5,F6,F7,F10	F2	140,113
<b>Amide (Self-loops)</b>								
1	Benzamide <sup>bc</sup>	122.060	C <sub>7</sub> H <sub>8</sub> NO	6.15	[M + H] <sup>+</sup>	F5,F1,F8,F10	F4	105,95,77
8	Cinnamide <sup>bc</sup>	148.076	C <sub>9</sub> H <sub>10</sub> NO	11.28	[M + H] <sup>+</sup>	F4,F8,F10,F10	F5	131,103
<b>Polyketides</b>								
21	Decarboxyportentol acetate <sup>b</sup>	331.188	C <sub>18</sub> H <sub>28</sub> O <sub>4</sub>	22.96	[M+Na] <sup>+</sup>	F1,F2,F3,F5,F8,F10	F2	173,147,137,109,95,83,69

Peak numbers correspond to the numbering of peaks that appear in the total ion chromatogram (TICs). <sup>a</sup> Structural hit obtained from GNPS spectral library matching. <sup>b</sup> Compounds have been elucidated from fractions (Figure 3). <sup>c</sup> Compounds previously reported in the leaves of *O. maingayi* [10]. <sup>d</sup> MS/MS spectra matched with published literature [22].

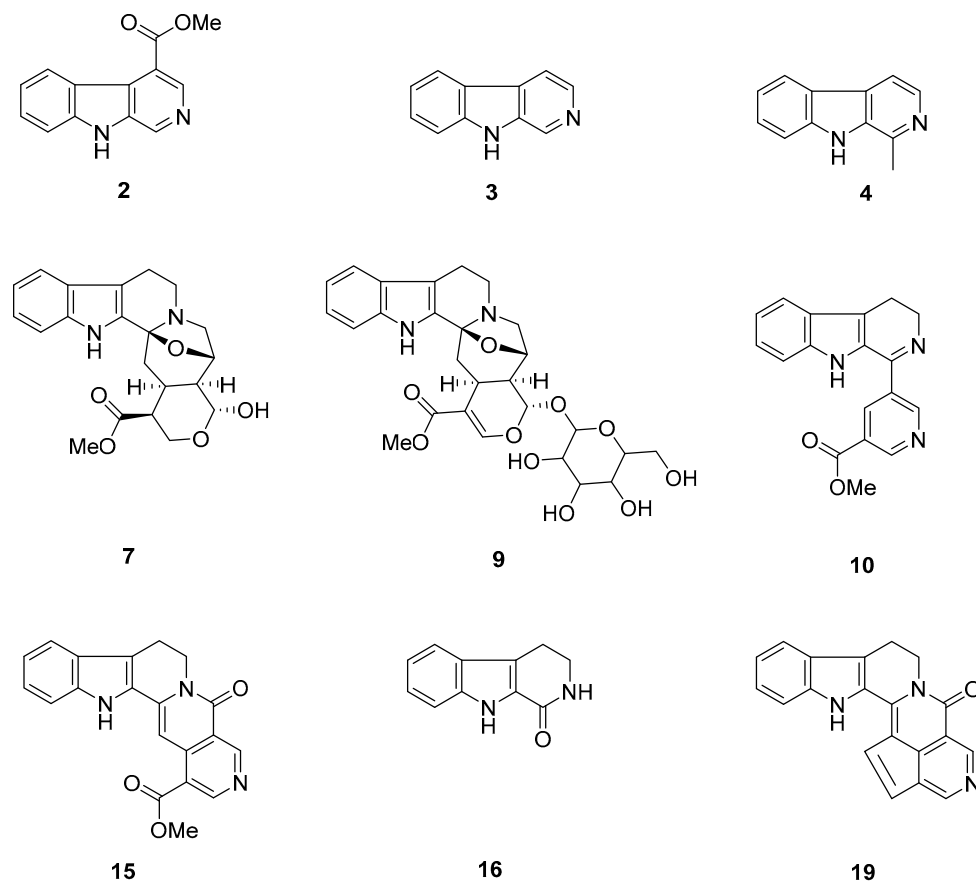


**Figure 3.** Compounds isolated from F5-F10: methyl 9H-β-carboline-4-carboxylate (2), norharmane (3), harmane (4), dihydrodeglycocadambine (7), cadambine (9), naucedine (10), neonaucledine (15), 1,2,3,4-tetranorharmane-1-one (16), and naulafine (19).

Dihydrodeglycocadambine **7** was obtained as an optically active, light yellow, and amorphous solid [ $\alpha$ ]<sub>D</sub><sup>25</sup> = +57.3 ( $c$  = 0.0004, MeOH), UV(MeOH)  $\lambda_{\max}$  (log  $\epsilon$ ) 222 (4.18), 274 (3.64) nm. It has the molecular formula C<sub>21</sub>H<sub>23</sub>N<sub>2</sub>O<sub>5</sub> as deduced from the LC-ESI-HR-MS/MS analysis [M + H]<sup>+</sup>, and  $m/z$  385.1754 (calcd. for C<sub>21</sub>H<sub>24</sub>N<sub>2</sub>O<sub>5</sub>, 385.1685) (Figure S1). The UV spectrum reveals a maximum absorption at  $\lambda_{\max}$  222 and 274 nm which reveals an indole chromophore [24], while the IR gives a broad band at 3339.6 cm<sup>-1</sup> due to O-H stretching and a sharp strong band at 1731.0 cm<sup>-1</sup> due to a C=O group. An analysis of the <sup>1</sup>H NMR (Figure S2) and HSQC (Figure S3) indicated four aromatics signal characteristic of unsubstituted indole moiety appearing at  $\delta_{\text{H}}$  7.74, (d,  $J$  = 7.7), H-9;  $\delta_{\text{H}}$  7.28, (t,  $J$  = 7.5), H-10;  $\delta_{\text{H}}$  7.34, (t,  $J$  = 7.4), H-11; and  $\delta_{\text{H}}$  7.67, (d,  $J$  = 8.1), H-12.

The <sup>13</sup>C NMR and DEPT (Figure S4 & Figure S5) indicate a total of twenty one carbons in the structure which belong to five quaternary carbons ( $\delta_{\text{C}}$  135.1, C-2; 92.3, C-3; 111.1, C-7; 127.2, C-8; and 138.4, C-13), nine methines ( $\delta_{\text{C}}$  119.9, C9; 119.7, C10; 122.7, C11; 111.4, C12; 29.8, C15; 48.9, C16; 74.8, C19; and 50.3, C20), five methylenes ( $\delta_{\text{C}}$  53.2, C-5; 22.8, C-6; 47.9, C-14; 67.8, C-17; and 57.3, C-18), one hemiacetal carbon ( $\delta_{\text{C}}$  97.1, C21), one methoxy group ( $\delta_{\text{C}}$  52.0, C-23), and one carbonyl groups ( $\delta_{\text{C}}$  173.0, C-22).

Further analysis of the <sup>1</sup>H and <sup>13</sup>C NMR spectroscopic data (Table 2) indicated that **7** was structurally related to **9**, except for the following two differences: firstly, the absence of glucosyl moiety at C-21, which suggested that **7** was the aglycone to **9**, and secondly the absent of double bond at C16-C17.

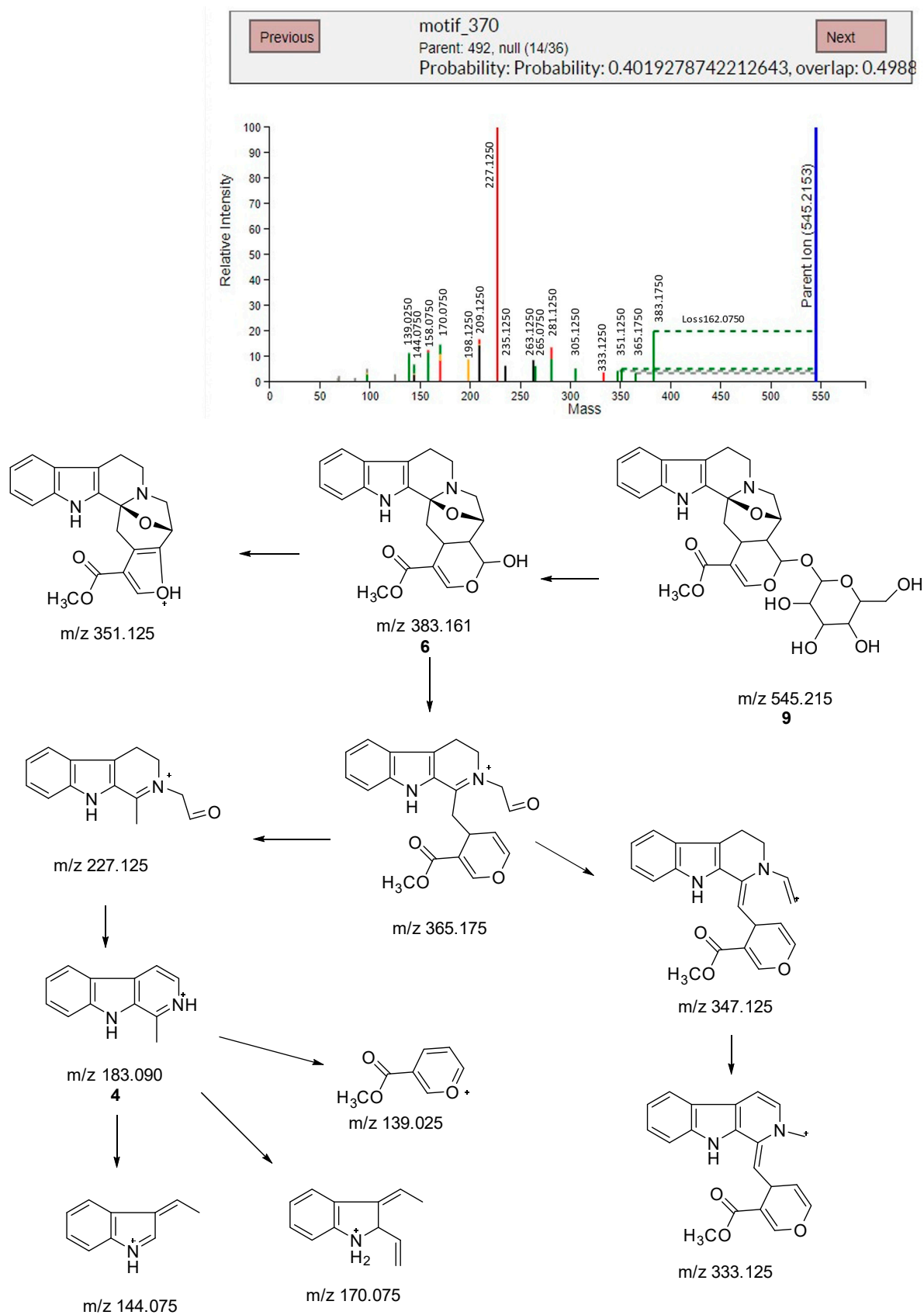
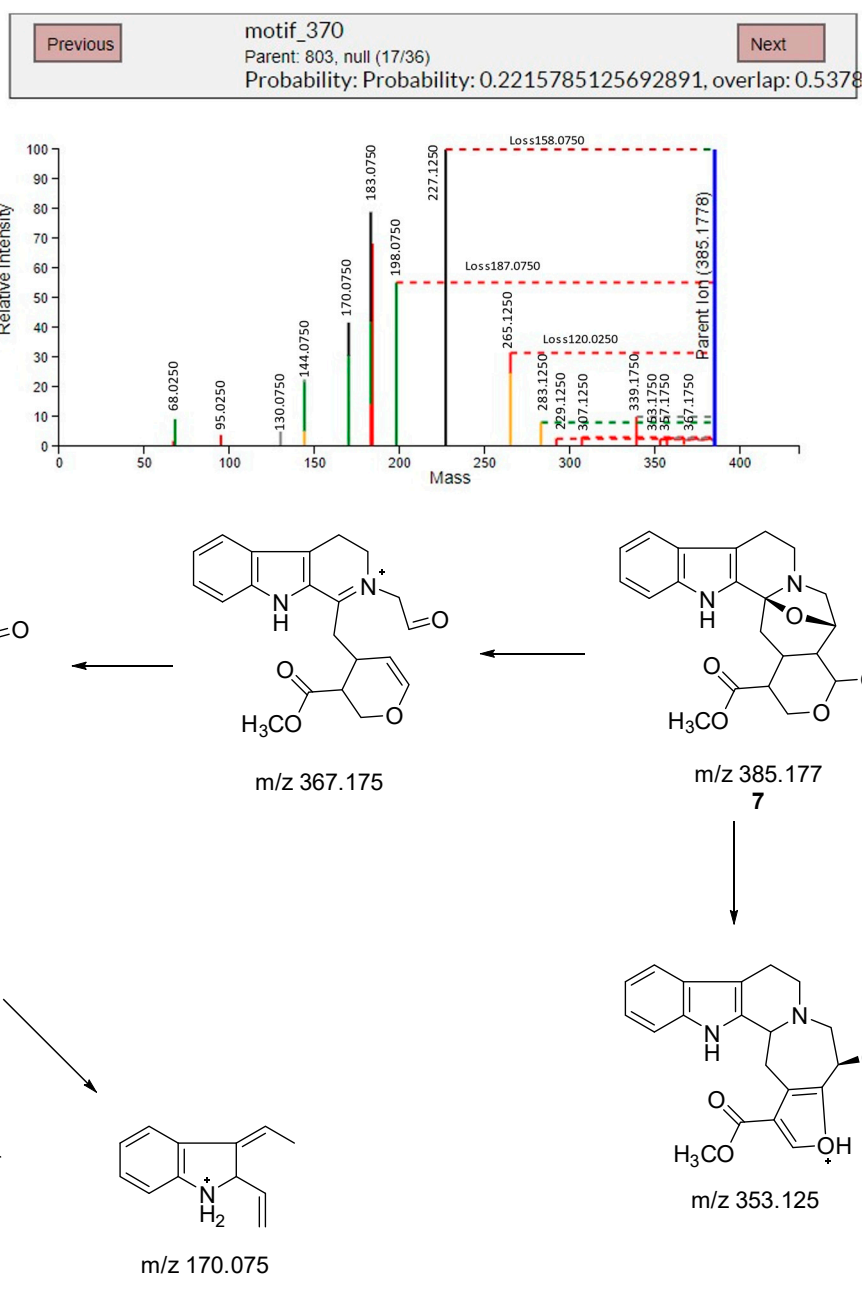


Figure 4. Mass spectra and fragmentation pathway of mass motif for parent 492.



**Figure 5.** Mass spectra and fragmentation pathway of mass motif for parent 830.

The location of the substituents and the ring arrangement were further confirmed by cross peaks in the HMBC spectra (Figure S6, Figure 6). The correlation of H-16/C-22 ( $\delta_c$  173.0), OMe-/C-22 ( $\delta_c$  173.0), and H-16/C-20 ( $\delta_c$  50.3) proves that the ester group is situated at  $\delta_c$  48.9, C-16. The cross peaks between H-17/C-21 ( $\delta_c$  97.1) and H-20/C-21 indicate the location of a hydroxyl group at C-21. Finally, the linkages between the rings C, D, E were assigned with the aid of the HMBC spectrum. The cross peak between H-18/C-5 and H-14/C-3 further confirms that the indole rings (A-C) and D are fused via a C-3-N-4 junction. The cross peak between H-18/C-20 and H-16/C-20 suggests that ring D is connected through a tetrahydropyran ring E through C-20.

**Table 2.** <sup>1</sup>H-NMR (600 MHz) and <sup>13</sup>C-NMR (150 MHz) spectral data of dihydrodeglycocadambine 7 in C<sub>5</sub>D<sub>5</sub>N.

Position	Dihydrodeglycocadambine 7		Cadambine 9		Cadambine [21]	
	$\delta_H$ ( <i>m, J</i> in Hz) in Pyridine, C <sub>5</sub> D <sub>5</sub> N	$\delta_C$ in Pyridine, C <sub>5</sub> D <sub>5</sub> N	$\delta_H$ ( <i>m, J</i> in Hz) in Pyridine, C <sub>5</sub> D <sub>5</sub> N	$\delta_C$ in Pyridine, C <sub>5</sub> D <sub>5</sub> N	$\delta_H$ ( <i>m, J</i> in Hz) in CD <sub>3</sub> OD	$\delta_C$ in CD <sub>3</sub> OD
NH	12.48 ( <i>br s</i> )					
2		135.1		134.6		133.2
3		92.3		92.1		93.0
5	2.83 ( <i>m</i> ) overlap 3.18 ( <i>d, J</i> = 8.1)	53.2	3.01 ( <i>m</i> ) 2.74 ( <i>m</i> ) 2.80 ( <i>m</i> )	53.0	3.16 ( <i>m</i> ) 2.79 ( <i>m</i> )	53.9
6	2.83 ( <i>m</i> ) overlap	22.8	4.63 ( <i>dd, J</i> = 3.0, 12.2)	22.8	2.80 <i>brs</i>	22.8
7		111.1		110.8		111.6
8		127.2		127.0		127.0
9	7.74 ( <i>d, J</i> = 7.6)	119.9	7.69 ( <i>d, J</i> = 7.7)	119.9	7.47 ( <i>d, J</i> = 7.8)	120.2
10	7.28 ( <i>t, J</i> = 7.6)	119.7	7.23 ( <i>t, J</i> = 7.7)	119.9	7.00 ( <i>t, J</i> = 7.8)	120.1
11	7.34 ( <i>t, J</i> = 7.6)	122.7	7.27 ( <i>t, J</i> = 7.7)	122.8	7.11 ( <i>t, J</i> = 7.8)	123.4
12	7.67 ( <i>d, J</i> = 7.6)	111.4	7.51 ( <i>d, J</i> = 7.7)	112.6	7.33 ( <i>d, J</i> = 7.8)	112.6
13		138.4		138.4		136.3
14a	2.28 ( <i>dd, J</i> = 12.0, 12.0)	47.9	2.38 ( <i>dd, J</i> = 5.9, 12.7)	44.1	2.06 ( <i>m</i> )	43.1
14b	2.09 ( <i>dd, J</i> = 12.0, 4.7)		2.33 ( <i>t, J</i> = 12.7)			
15	2.83 ( <i>m</i> ) overlap	29.8	3.48 ( <i>m</i> )	26.41	3.26 ( <i>m</i> )	26.9
16	2.65 ( <i>m</i> )	48.9		110.8		111.3
17a	4.33 ( <i>dd, J</i> = 11.2, 4.3)					
17b	3.97 ( <i>t, J</i> = 11.2)	67.8	7.65 ( <i>s</i> )	153.4	7.57 <i>s</i>	154.4
18a	2.83 ( <i>m</i> ) overlap		3.14 ( <i>d, J</i> = 10.2)		3.51 ( <i>brd, J</i> = 10.8)	
18b	2.62 ( <i>d, J</i> = 10.1)	57.3	2.86 ( <i>m</i> )	59.4	3.02 ( <i>dd, J</i> = 10.8, 7.3)	59.4
19	5.22 ( <i>dd, J</i> = 6.2, 2.0)	74.8	5.10 ( <i>d, J</i> = 7.0)	73.8	4.94 ( <i>brd, J</i> = 7.3)	74.6
20	2.20 ( <i>m</i> )	50.3	1.78 ( <i>t, J</i> = 7.0)	40.9	1.76 ( <i>m</i> )	41.1
21	5.04 ( <i>d, J</i> = 8.6)	97.1	5.82 ( <i>d, J</i> = 9.2)	98.2	5.84 ( <i>d, J</i> = 9.3)	97.6
22-C=O		173.0		167.6		168.9
23-OCH <sub>3</sub>	3.49 ( <i>s</i> )	52.0	3.60 ( <i>bs</i> )	51.5	3.65 <i>s</i>	51.9
1'			5.19 ( <i>d, J</i> = 7.8)	103.0	4.80 <i>d, J</i> = 7.9	101.7
2'			4.16 ( <i>m</i> )	75.4	3.30 ( <i>m</i> )	74.9
3'			4.30 ( <i>t, J</i> = 8.9)	78.0	3.42 <i>t, J</i> = 9.0	78.1
4'			4.20 ( <i>m</i> )	72.4	3.28 ( <i>m</i> )	71.7
5'			3.97 ( <i>ddd, J</i> = 2.4, 7.0)	79.0	3.34 ( <i>m</i> )	78.5
6'			4.48 ( <i>dd, J</i> = 11.8, 2.4) 4.17 ( <i>m</i> ) overlapp	63.6	3.87 ( <i>dd, J</i> = 12.1, 2.3) 3.61 ( <i>dd, J</i> = 12.1, 6.4)	62.9

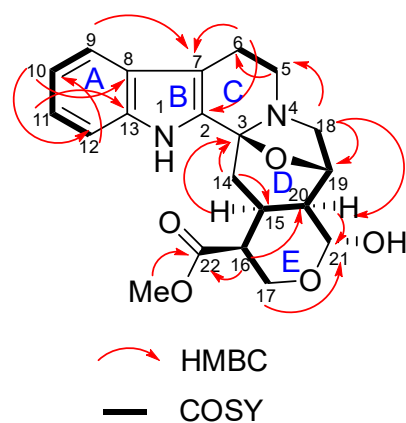


**Figure 6.** Selected key correlation of dihydrodeglycocadambine 7.

The relative stereochemistry of **7** was confirmed from the NOESY spectrum and correlation (Figure S7, Figure 7) by comparison of its correlations with those of a similar skeleton [21]. The stereochemistry at C-20 could be ascertained by the NOESY relationship between H19 and H-20. The presence of a chiral carbon at C-19 as indicated by the *O*-bridged complex between C-3 and C-19 exists as a  $\beta$ -configuration. This  $\beta$ -configuration leads to the assignment of the proton at C-19 as an  $\alpha$ -configuration. The NOESY spectrum of H-19 correlates with H-20 as an  $\alpha$ -configuration. In addition, H-20 correlates with H-21 in the COSY spectrum (Figure S8); however, there is no correlation between H-20 and H-21 in the NOESY spectrum. Thus, it can be deduced that H-21 has a different configuration than H-20 and is assigned as a  $\beta$ -configuration. There are two geminal protons for C-17 (H17 $\alpha$  and H17 $\beta$ ). H-17 $\beta$  shows correlation with H-21 $\beta$ . It also proves that H16 exists as an  $\alpha$ -configuration due to the direct correlation of H17 $\alpha$  and H16 $\alpha$ . There is a direct correlation between H-15 and H-16 and between H-15 and H-20; therefore, we can presume that H-15 also exists as  $\alpha$ -oriented.

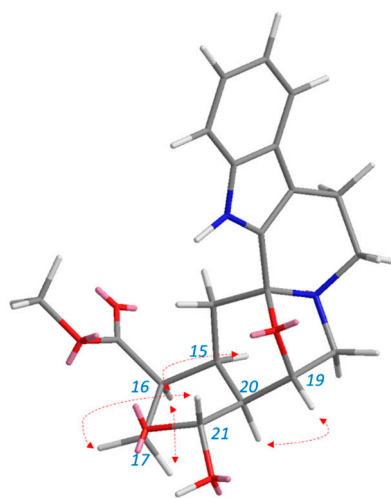


**Figure 7.** Selected NOESY correlation of dihydrodeglycocadambine **7**.

The  $^1\text{H}$  NMR and  $^{13}\text{C}$  NMR (600 MHz) spectral assignments performed by extensive 2D-NMR experiments (COSY, HSQC and HMBC) are summarized in Figure 6 and Table 2.

#### 4. Conclusions

The combination of MN, analysis of the fragmentation patterns, and manual dereplication proved to be a useful strategy for facilitating dereplication of IA scaffold from *O. maingayi*. The MN not only aided the detection of the presence of the new compound, dihydrodeglycocadambine **7**, but also enabled the selection of fractions containing the targeted compounds, as well as the detection and identification of known IA scaffold. A total of nine indole alkaloids, two coumarins, and one fatty acid were positively identified in the bark of *O. maingayi*. Moreover, several clusters contain ions that could not be annotated, suggesting that they may also possess novel compounds that are yet to be discovered.

**Supplementary Materials:** The following supporting information can be downloaded at <https://www.mdpi.com/article/10.3390/separations10020074/s1>. Figure S1: LCMS of Dihydrodeglycocadambine (**7**); Figure S2:  $^1\text{H}$  NMR spectrum (600 MHz,  $\text{C}_5\text{D}_5\text{N}$ ) of Dihydrodeglycocadambine (**7**); Figure S3: HSQC spectrum (600 MHz,  $\text{C}_5\text{D}_5\text{N}$ ) of Dihydrodeglycocadambine (**7**); Figure S4:  $^{13}\text{C}$  NMR spectrum (600 MHz,  $\text{C}_5\text{D}_5\text{N}$ ) of Dihydrodeglycocadambine (**7**); Figure S5: DEPT 90 spectrum (600 MHz,  $\text{C}_5\text{D}_5\text{N}$ ) of Dihydrodeglycocadambine (**7**); Figure S6: HMBC spectrum (600 MHz,  $\text{C}_5\text{D}_5\text{N}$ ) of Dihydrodeglycocadambine (**7**); Figure S7: NOESY spectrum (600 MHz,  $\text{C}_5\text{D}_5\text{N}$ ) of Dihydrodeglycocadambine (**7**); Figure S8: COSY spectrum (600 MHz,  $\text{C}_5\text{D}_5\text{N}$ ) of Dihydrodeglycocadambine (**7**).

**Author Contributions:** N.O. and A.Z. contributed to the experiments and analyses, participated in the discussion of results, and wrote the manuscript; K.A. participated in material preparation and

manuscript writing; H.H., N.E.R. and N.H.I. participated in experiments; W.N.N.W.O., P.C., M.A.B. and M.L. provided intellectual input in the analysis of the results. All authors have read and agreed to the published version of the manuscript.

**Funding:** This work was financially supported by the Ministry of Higher Education (MOHE) under the Fundamental Research Grant Scheme (FRGS) FRGS/1/2020/SKK0/UM/01/5; FP054-2020, and the University of Malaya Research Fund Assistance (BKP) BK040-2017.

**Data Availability Statement:** Not applicable.

**Acknowledgments:** The authors disclosed receipt of the following financial support for the travel grant in studies molecular networking through a French–Malaysian Collaborative grant on Phytochemical Analysis on Malayan Flora, project number 57-02-03-1007 and Embassy of France in Malaysia.

**Conflicts of Interest:** The authors declare no conflict of interest.

## References

1. O'Connor, S.E.; Maresh, J.J. Chemistry and biology of monoterpene indole alkaloid biosynthesis. *Nat. Prod. Rep.* **2006**, *23*, 532–547. [[CrossRef](#)] [[PubMed](#)]
2. Szabó, L.F. Rigorous Biogenetic Network for a Group of Indole Alkaloids Derived from Strictosidine. *Molecules* **2008**, *13*, 1875–1896. [[CrossRef](#)] [[PubMed](#)]
3. Škubník, J.; Pavlíčková, V.S.; Ruml, T.; Rimpelová, S. Vincristine in Combination Therapy of Cancer: Emerging Trends in Clinics. *Biology* **2021**, *10*, 849. [[CrossRef](#)] [[PubMed](#)]
4. Shamon, S.D.; Perez, M. Blood pressure-lowering efficacy of reserpine for primary hypertension. *Cochrane Database Syst. Rev.* **2016**, *12*, Cd007655. [[CrossRef](#)]
5. Rtibi, K.; Grami, D.; Selmi, S.; Amri, M.; Sebai, H.; Marzouki, L. Vinblastine, an anticancer drug, causes constipation and oxidative stress as well as others disruptions in intestinal tract in rat. *Toxicol. Rep.* **2017**, *4*, 221–225. [[CrossRef](#)]
6. Dalal, N.; Ravishankar, R. In vitro propagation of *Ochreinauclea missionis* (Wall. EX G. Don), an ethnomedicinal endemic and threatened tree. *Vitr. Cell. Dev. Biol. Plant* **2001**, *37*, 820–823. [[CrossRef](#)]
7. Ravishankar, R. Genetic fidelity in micropropagated plantlets of *Ochreinauclea missionis* an endemic, threatened and medicinal tree using ISSR markers. *Afr. J. Biotechnol.* **2009**, *8*, 2933–2938.
8. Ridsdale, C.E. A revision of the tribe Naucleaeae s.s. (Rubiaceae). *Blumea Biodivers. Evol. Biogeogr. Plants* **1978**, *24*, 307–366.
9. Lim, S.C.; Gan, K.S.; Choo, K.T. Identification and utilisation of lesser-known commercial timbers in Peninsular Malaysia 1: Ara, Bangkal, Bebusok and Bekoi. Timber Technology Centre (TTC), FRIM, Kuala Lumpur. *Timber Tech. Bull.* **2004**, *29*, 139–258.
10. Mukhtar, M.R.; Osman, N.; Awang, K.; Hazni, H.; Qureshi, A.K.; Hadi, A.H.; Zaima, K.; Morita, H.; Litaudon, M. Neonaucleine, a new indole alkaloid from the leaves of *Ochreinauclea maingayii* (Hook. f.) Ridsd. (Rubiaceae). *Molecules* **2011**, *17*, 267–274. [[CrossRef](#)]
11. Pluskal, T.; Castillo, S.; Villar-Briones, A.; Orešič, M. MZmine 2: Modular framework for processing, visualizing, and analyzing mass spectrometry-based molecular profile data. *BMC Bioinform.* **2010**, *11*, 395. [[CrossRef](#)] [[PubMed](#)]
12. van Der Hooft, J.J.; Wandy, J.; Barrett, M.P.; Burgess, K.E.; Rogers, S. Topic modeling for untargeted substructure exploration in metabolomics. *Proc. Natl. Acad. Sci. USA* **2016**, *113*, 13738–13743. [[CrossRef](#)] [[PubMed](#)]
13. Chambers, M.C.; Maclean, B.; Burke, R.; Amodei, D.; Ruderman, D.L.; Neumann, S.; Gatto, L.; Fischer, B.; Pratt, B.; Egertson, J.; et al. A cross-platform toolkit for mass spectrometry and proteomics. *Nat. Biotechnol.* **2012**, *30*, 918–920. [[CrossRef](#)] [[PubMed](#)]
14. Wang, M.; Carver, J.J.; Phelan, V.V.; Sanchez, L.M.; Garg, N.; Peng, Y.; Nguyen, D.D.; Watrous, J.; Kapono, C.A.; Luzzatto-Knaan, T.; et al. Sharing and community curation of mass spectrometry data with Global Natural Products Social Molecular Networking. *Nat. Biotechnol.* **2016**, *34*, 828–837. [[CrossRef](#)] [[PubMed](#)]
15. Otasek, D.; Morris, J.H.; Bouças, J.; Pico, A.R.; Demchak, B. Cytoscape Automation: Empowering workflow-based network analysis. *Genome Biol.* **2019**, *20*, 185. [[CrossRef](#)]
16. Wandy, J.; Zhu, Y.; van der Hooft, J.; Daly, R.; Barrett, M.P.; Rogers, S. Ms2lda.org: Web-based topic modelling for substructure discovery in mass spectrometry. *Bioinformatics* **2017**, *34*, 317–318. [[CrossRef](#)]
17. Repke, D.B.; Jahangir; Clark, R.D.; Nelson, J.T.; MacLean, D.B. Synthesis of nauclefine, angustidine, angustine, (±)-13b,14-dihydro-angustine and naulafine. *Tetrahedron* **1989**, *45*, 2541–2550. [[CrossRef](#)]
18. Parameswaran, P.S.; Naik, C.G.; Hegde, V.R. Secondary Metabolites from the Sponge *Tedania anhelans*: Isolation and Characterization of Two Novel Pyrazole Acids and Other Metabolites. *J. Nat. Prod.* **1997**, *60*, 802–803. [[CrossRef](#)]
19. Seki, H.; Hashimoto, A.; Hino, T. The <sup>1</sup>H- and <sup>13</sup>C-Nuclear Magnetic Resonance Spectra of Harman. Reinvestigation of the Assignments by One- and Two-Dimensional Methods. *Chem. Pharm. Bull.* **1993**, *41*, 1169–1172. [[CrossRef](#)]
20. Lai, Z.-Q.; Liu, W.-H.; Ip, S.-P.; Liao, H.-J.; Yi, Y.-Y.; Qin, Z.; Lai, X.-P.; Su, Z.-R.; Lin, Z.-X. Seven Alkaloids from *Picrasma quassioides* and Their Cytotoxic Activities. *Chem. Nat. Compd.* **2014**, *50*, 884–888. [[CrossRef](#)]

21. Yuan, H.-L.; Zhao, Y.-L.; Qin, X.-J.; Liu, Y.-P.; Yu, H.-F.; Zhu, P.-F.; Jin, Q.; Yang, X.-W.; Luo, X.-D. Anti-inflammatory and analgesic activities of *Neolamarckia cadamba* and its bioactive monoterpene indole alkaloids. *J. Ethnopharmacol.* **2020**, *260*, 113103. [[CrossRef](#)] [[PubMed](#)]
22. Wu, X.-D.; Wang, L.; He, J.; Li, X.-Y.; Dong, L.-B.; Gong, X.; Gao, X.; Song, L.-D.; Li, Y.; Peng, L.-Y.; et al. Two New Indole Alkaloids from *Emmenopterys henryi*. *Helvetica Chim. Acta* **2013**, *96*, 2207–2213. [[CrossRef](#)]
23. Gai, Y.; Chen, H.; Wu, C.; Feng, F.; Wang, Y.; Liu, W.; Wang, S. Analysis of the traditional medicine YiGan San by the fragmentation patterns of cadambine indole alkaloids using HPLC coupled with high-resolution MS. *J. Sep. Sci.* **2013**, *36*, 3723–3732. [[CrossRef](#)] [[PubMed](#)]
24. Albinsson, B.; Norden, B. Excited-state properties of the indole chromophore: Electronic transition moment directions from linear dichroism measurements: Effect of methyl and methoxy substituents. *J. Phys. Chem.* **1992**, *96*, 6204–6212. [[CrossRef](#)]

**Disclaimer/Publisher’s Note:** The statements, opinions and data contained in all publications are solely those of the individual author(s) and contributor(s) and not of MDPI and/or the editor(s). MDPI and/or the editor(s) disclaim responsibility for any injury to people or property resulting from any ideas, methods, instructions or products referred to in the content.